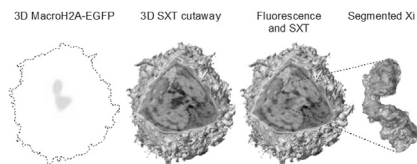


(CCFT-SXT). Correlation of these two three-dimensional datasets was performed using fiducial markers visible in both modalities. The Xi was identified in each cell by its strong enrichment in a fluorescently-labeled histone variant, macroH2A-EGFP. We present the overall topology, compaction profile, and volume occupied by the Xi in interphase nuclei. Physical contacts with nucleoli and the nuclear envelope are also described. Examination of eleven individual cells showed that there is considerable variation in the spatial arrangement and compaction profile adopted by the Xi.



## 2198-Plat

### Observation of the Change of Synapses After Long-Term Potentiation Induction using Super-Resolution Imaging

Sang Hak Lee<sup>1,2</sup>, En Cai<sup>1,2</sup>, Okunola Jeyifous<sup>3</sup>, Michelle A. Baird<sup>4</sup>, Michael W. Davidson<sup>4</sup>, William N. Green<sup>3</sup>, Paul R. Selvin<sup>1,2</sup>.

<sup>1</sup>University of Illinois at Urbana-Champaign, Urbana, IL, USA, <sup>2</sup>Center for the Physics of Living Cells, University of Illinois at Urbana-Champaign, Urbana, IL, USA, <sup>3</sup>University of Chicago, Chicago, IL, USA, <sup>4</sup>Florida State University, Tallahassee, FL, USA.

Synapses are the fundamental structures for signal transmission in neurons. A synapse is a cell-cell junction composed of pre-synapse and post-synapse between neurons. The structure of synapses is dynamically changing upon external stimuli. In this work, we used super-resolution imaging technique (PALM) to study the synaptic changes after inducing long-term potentiation (LTP). In particular, after LTP induction, we investigated the changes in distances between 1. A presynaptic protein (synapsin and postsynaptic scaffold proteins (Homer1 and PSD95) and 2. Two different postsynaptic scaffold proteins, namely Homer1 and PSD95. We labeled these proteins using photo-activable proteins such as mEOS2, Dronpa, and mGeos, and obtained two-color PALM imaging for each pair of synaptic proteins. Chromatic aberration was corrected for a more precise measurement of the distances. We found out that, after LTP induction, the distance between Homer1 and PSD95 decreased significantly from 330 nm to 90 nm; the distance between synapsin and PSD95 also decreased from 243 nm to 125 nm. Moreover, we carried out fast PALM imaging, which allows us to take super-resolution images every minute, in order to observe the volume change of synapses during LTP. Observation of the time-dependent distribution of PSD95 and Homer1 has shown that the average volume of synapses is increasing after LTP induction from 0.05  $\mu\text{m}^3$  to 0.076  $\mu\text{m}^3$ .

## 2199-Plat

### Single-Molecule Fluorescence Imaging Reveals Mismatch Repair Dynamics in Live *Bacillus Subtilis*

Yi Liao<sup>1</sup>, Jeremy W. Schroeder<sup>2</sup>, Lyle A. Simmons<sup>2</sup>, Julie S. Biteen<sup>1</sup>.

<sup>1</sup>Chemistry, University of Michigan, Ann Arbor, MI, USA, <sup>2</sup>Molecular, Cellular and Developmental Biology, University of Michigan, Ann Arbor, MI, USA.

The error-free progression of DNA replication is essential for all organisms, and deficiencies in DNA repair mechanisms can have severe consequences, from increased antibiotic resistance in bacteria to human cancers. The mismatch repair (MMR) pathway corrects base-pairing errors that are incorporated during genome replication. This pathway is critical for maintaining genomic fidelity: loss of MMR increases the mutation rate several hundred-fold in bacteria and humans alike. From prokaryotes to human cells, the highly conserved MMR protein MutS and its homologs recognize mismatched nucleotides and recruits downstream MMR proteins for repair. Despite the crucial role of MutS in MMR, the mechanism by which MutS first locates base-pairing errors remains unclear.

We have developed new methods of super-resolution imaging to reveal the in vivo single-molecule distributions and dynamics of MutS in live *Bacillus subtilis*. This Gram-positive bacterium has served as the model for studying DNA replication and repair due to its genetic competence and high homology with corresponding pathways in humans. Based on Photoactivated Localization Microscopy (PALM) and single-particle tracking (SPT), we localized and tracked MutS-PAmCherry and the replisome subunit DnaX-mCitrine with 20-nm precision to reveal the spatial relationship and diffusive behaviors of these two proteins. We observed transient, mismatch-dependent colocalization between MutS-PAmCherry and DnaX-mCitrine with two-color PALM imaging, and SPT revealed dramatic changes in MutS-PAmCherry diffusion rates and confinement behavior upon mutagen treatment. To develop a mechanistic understanding, we have studied wt MutS as well as mutant strains defective for mismatch recognition and mismatch unbinding, respectively, and studied

how the interactions between MutS-PAmCherry and the replisome are changed by such mutations. Together, our results provide strong evidence supporting that MutS recruitment to the replisome is required for MMR and precedes mismatch binding events in vivo.

## 2200-Plat

### Subdiffraction Imaging Reveals Molecular Architecture at the Transition Zone of Primary Cilia

T. Tony Yang<sup>1</sup>, Won-Jing Wang<sup>2</sup>, Arthi Suresh<sup>1</sup>, Meng-Fu Bryan Tsou<sup>2</sup>, Jung-Chi Liao<sup>1,3</sup>.

<sup>1</sup>Mechanical Engineering, Columbia University, New York, NY, USA, <sup>2</sup>Cell Biology Program, Memorial Sloan-Kettering Cancer Center, New York, NY, USA, <sup>3</sup>Biomedical Engineering, Columbia University, New York, NY, USA. Recent studies have identified important regulating elements for transition zone (TZ) gating in cilia. However, the architecture of the TZ region and its arrangement relative to intraflagellar transport (IFT) proteins remain largely unknown, hindering the mechanistic understanding of the regulation mechanisms. One of the major challenges comes from the tiny volume at the ciliary base packed with numerous proteins, with the diameter of the TZ close to the diffraction limit of conventional microscopes. Using a custom-built stimulated emission depletion (STED) superresolution microscope, we revealed relative localizations of TZ proteins, IFT proteins, transition fiber (TF) proteins, and centriole proteins. We found TCTN2 at the outmost periphery of the TZ close to the ciliary membrane, with a  $227 \pm 18$  nm diameter. TMEM67 was adjacent to TCTN2, with a  $205 \pm 20$  nm diameter. RPGRIP1L was localized toward the axoneme at the same axial level as TCTN2 and TMEM67, with a  $165 \pm 8$  nm diameter. Surprisingly, CEP290 (antibody against C-terminal amino acids) was localized at the proximal side of the TZ close to the distal end of the centrin-labeled basal body. The lateral width was unexpectedly close to the width of the basal body, distant from the potential Y-links region of the TZ. IFT88 was also surprisingly distributed in two distinct patterns, forming three puncta or a Y shape at the ciliary base. We hypothesize that the two distribution states of IFT88 correspond to the open and closed gating states of the TZ, where IFT particles aggregate to form three puncta when the gate is closed, and move to form the branches of the Y-shape pattern when the gate is open.

## 2201-Plat

### Super-Resolution Imaging of Telomeres Reveals that Compaction of Telomeric DNA by Shelterin Protects Chromosome Terminii

Jigar N. Bandaria<sup>1</sup>, Veysel Berk<sup>2</sup>, Steven Chu<sup>2</sup>, Ahmet Yildiz<sup>1</sup>.

<sup>1</sup>Physics and Molecular and Cell Biology, University of California, Berkeley, CA, USA, <sup>2</sup>Physics and Molecular and Cellular Physiology, Stanford University, Stanford, CA, USA.

Telomeres, which are tandem TTAGGG repeats at the ends of mammalian chromosomes, are susceptible to degradation by nucleases and misrecognition as breaks in DNA. Telomeres are protected against DNA damage response (DDR) pathways by the shelterin complex. It has been proposed that higher order remodeling of telomeric chromatin by shelterin plays a role in this protection, but telomeres cannot be studied by crosslinking and chromosome capture methods due to failure of sequence discrimination between repetitive TTAGGG tracts. Using photoactivated localization microscopy (PALM) we imaged telomeres in human cells at  $\sim 15$  nm of resolution. We found that shelterin mediates formation of compact telomeric structures ( $\sim 150$  nm in diameter). Knockdown of TRF1, TRF2 and TIN2 subunits of shelterin results in decompaction and up to 30-fold increase in volume of these telomeric structures. Mutations that abrogate TRF1 or TRF2 dimerization also lead to different levels of telomere decompaction, which positively correlates with DDR signal accumulation at telomeres in these cells. The changes in telomere structure are not due to DDR accumulation in TRF2 mutant cells, because similar levels of decompaction are observed after inactivating the ataxia telangiectasia mutated (ATM) pathway using RNAi. Our results demonstrate that shelterin remodels telomeric chromatin into compact structures by inter-repeat crosslinking of telomeric tracts.

## 2202-Plat

### Live 4D Imaging of the Embryonic Vertebrate Heart with Two-Photon Light Sheet Microscopy and Simultaneous Optical Phase Stamping

Thai V. Truong<sup>1</sup>, Vikas Trivedi<sup>2</sup>, Le Trinh<sup>1</sup>, Daniel Holland<sup>1</sup>, Francesco Cutrale<sup>1</sup>, John M. Choi<sup>1</sup>, Scott E. Fraser<sup>1</sup>.

<sup>1</sup>Translational Imaging Center, University of Southern California, Los Angeles, CA, USA, <sup>2</sup>Bioengineering, California Institute of Technology, Pasadena, CA, USA.

The developing vertebrate heart is a highly dynamic organ that starts to function early on during embryonic development, even as it continues to undergo dramatic morphological changes and cellular differentiation. Fast and high resolution three-dimensional (3D) imaging is needed to document the intrinsic

cellular dynamics of the beating heart, as a critical step in understanding its development. To meet the challenges of obtaining sub-cellular resolution imaging of a dynamic 100-micron length scale 3D structure, which moves quasi-periodically at frequency of a few Hertz, over tens of microns amplitude, we have employed two-photon light sheet microscopy (2p-SPIM) and a novel independent optical phase stamping method to generate well-resolved 3D movies (4D) of the beating heart. Applying this 4D imaging modality to zebrafish embryos, we have found remarkable heterogeneity in cardiomyocyte morphology, gene expression, and behavior both during the cardiac cycle, and over the developmental time. The observed heterogeneity appears to play a key role in the maintenance of tissue geometry and cardiac output as the heart undergoes cycles of contraction and expansion. The variation in cellular morphology and behavior provide new insights into the tight link between cellular dynamics, mechanical environment exerted and felt by the beating heart, and the genetic program that governs not only the differentiation and construction but also the maintenance of this important organ.

## 2203-Plat

### Structurally Distinct $\text{Ca}^{2+}$ Domains of Sperm Flagella Modulate Hyperactivated Motility

Sang-Hee Shim<sup>1</sup>, Jean-Ju Chung<sup>2,3</sup>, Xiaowei Zhuang<sup>1,4</sup>, David E. Clapham<sup>2,3</sup>.

<sup>1</sup>Department of Chemistry and Chemical Biology, Harvard University, Cambridge, MA, USA, <sup>2</sup>Department of Neurobiology, Harvard Medical School, Boston, MA, USA, <sup>3</sup>Department of Cardiology, Children's Hospital, Boston, MA, USA, <sup>4</sup>Department of Physics, Harvard University, Cambridge, MA, USA.

Mammalian sperm cells must swim long distances to fertilize the egg. The powerful burst of hyperactivated motility, which is necessary for successful fertilization, requires calcium influx via CatSper, sperm flagellar  $\text{Ca}^{2+}$  channel. We characterized ultrastructures of CatSper channels and  $\text{Ca}^{2+}$  signaling molecules in single flagella. We find that the CatSper channel, together with other signaling molecules, organizes four linear  $\text{Ca}^{2+}$  domains along the flagella. This unique structure focuses tyrosine phosphorylation in time and space during capacitation. We looked for motility-correlative molecular phenotypes in capacitation-induced heterogeneous sperm populations. Hyperactivated motility correlates with the intact CatSper domains, the presence of P-Tyr, and the efficient sperm migration in female reproductive tract. Our results offer a new view of spatiotemporal organization of signal transduction in flagella that augments the mechanistic insights of  $\text{Ca}^{2+}$  in motility regulation for mammalian spermatozoa.

## Platform: Voltage-gated K Channels: Mostly BK and Structure Function

## 2204-Plat

### Location of BK Ion Permeation Gate Revealed by $\text{Cd}^{2+}$ -Cys Coordination in the BK Inner Pore Region

Yu Zhou, Christopher Lingle.

Washington University School of Medicine, St. Louis, MO, USA.

The BK-type potassium channels contains a  $\text{K}^{+}$ -selective ion permeation pathway that opens and closes in response to changes of transmembrane voltage or intracellular  $\text{Ca}^{2+}$  concentration. Previous studies using large probes such as cytosolic blockers and MTS reagents have suggested that, unlike the voltage-gated potassium (Kv) channels, the BK ion permeation gate may not reside at the cytosolic entrance of the pore. However, this issue remains incompletely resolved. Here we utilize  $\text{Cd}^{2+}$ , a probe of comparable sizes to  $\text{K}^{+}$ , to further test state-dependent access to the BK inner cavity. We introduced cysteines at A316, a BK pore lining position inside the proposed Kv cytosolic gate, and determined  $\text{Cd}^{2+}$ -Cys coordinating rate at this position in both open and closed states. The result shows that the state-dependence of coordination between  $\text{Cd}^{2+}$  and A316C is moderate, with coordinating rate less than 10 times faster in the open state. In addition, the coordinating rate of A316C with  $\text{Cd}^{2+}$  in a closed BK channel is comparable to that of an inner cavity cysteine (I361C) with  $\text{Cd}^{2+}$  in an open CNG channel. We also examined  $\text{Cd}^{2+}$ -Cys coordination in the YVP motif (V319C) near the cytosolic entrance of the pore. The counterpart region in Kv channel forms a tight steric exclusion when channel is closed. As a result, the homologous site of V319 in Kv channel (V474) is not accessible to  $\text{Cd}^{2+}$  in closed state. In BK channel,  $\text{Cd}^{2+}$  coordinates with V319C in both open and closed states, with open-state coordinating rate less than 1-fold faster than that of closed-state coordinating rate. These results suggest that the BK ion permeation gate is not located at its cytosolic entrance. Instead, the selectivity filter is the only possible region in BK to control ion flow.

## 2205-Plat

### Identification of a Discrete Alcohol-Sensing Site in the BK (SLO1) Channel

Anna Bukiya, Justin Edwards, Alex Dopico.

Pharmacology, The University of Tennessee Hlth. Sci. Ctr., Memphis, TN, USA.

In both mammals and non-mammalian models, exposure of BK (slo1) channels to ethanol concentrations reached in circulation during alcohol intoxication (10-100 mM) leads to changes in channel steady-state activity (NPo) and thus, perturbation of physiology and behavior (reviewed in: Brodie *et al.*, 2007; Treisman & Martin, 2009; Dopico *et al.*, 2012). Site(s) and mechanism(s) participating in ethanol-slo1 channel interactions are unknown. Using patch-clamp recording, point mutagenesis and computational modeling based on crystallographic data, we unveil that ethanol docks onto a water-accessible site that is strategically positioned between the slo1 calcium-sensors and gate. Ethanol only accesses this site in the presence of calcium, the slo1 channel's primary physiological agonist. Within the site, ethanol hydrogen-bonds with Lys361. Moreover, substitutions that frustrate this bonding (K361N) or prevent ethanol molecules from accessing Lys361 (S357Y) abolish alcohol action on slo1 NPo without altering basal channel function. After creating n-alkanol conformational libraries and using a docking routine to find representative poses for the n-alkanol molecules, we estimate that site dimensions are:  $7.5 \times 7.5 \times 10 \text{ \AA}$ , this site accommodating effective (ethanol-heptanol) but not ineffective (octanol, nonanol) slo1 channel activators. This study presents: i) the first identification and characterization of an n-alkanol recognition site in a member of the voltage-gated TM6 channel superfamily; ii) structural insights on ethanol allosteric interactions with ion-gated ion channels, and iii) a first step for designing agents that antagonize BK channel-mediated alcohol actions without perturbing basal channel function. Support: R37AA11560 (AMD).

## 2206-Plat

### Baseline Properties of Slo1 $\text{K}^{+}$ (BK) Channels Without the Gating Ring

Yanyan Geng<sup>1</sup>, Gonzalo Budelli<sup>2</sup>, Alice Butler<sup>2</sup>, Celia Santi<sup>2</sup>, Juan Ferreira<sup>2</sup>, Lawrence Salkoff<sup>2</sup>, Karl L. Magleby<sup>1</sup>.

<sup>1</sup>Department of Physiology and Biophysics, University of Miami Miller School of Medicine, Miami, FL, USA, <sup>2</sup>Department of Anatomy & Neurobiology, Washington University School of Medicine, St. Louis, MO, USA. High conductance  $\text{Ca}^{2+}$ - and voltage-activated  $\text{K}^{+}$  (Slo1 or BK) channels have two functional domains: a "core" consisting of four voltage sensors controlling an ion-conducting pore, and a larger "tail" that forms an intracellular gating ring thought to confer  $\text{Ca}^{2+}$  and  $\text{Mg}^{2+}$  sensitivity. Whereas the modular structure is known, the properties of the individual modules and the transduction pathways among the modules are poorly understood because it has not been possible to study the core in isolation. To approach this problem, we developed novel constructs that allow functional cores of Slo1 channels to be expressed in the absence of the gating ring. One of these constructs replaced the 827 amino acid gating ring with a short synthetic peptide of 11 amino acids to enhance synthesis and surface expression. Functional expression of this construct in *Xenopus* oocytes produced currents from channels that: displayed voltage activation with a right-shifted G-V relation; lacked  $\text{Ca}^{2+}$  and  $\text{Mg}^{2+}$  sensitivity; exhibited a six-fold reduction in mean open interval and burst duration; had an apparent ~30% reduction in single-channel conductance; and were blocked by extracellular iberiotoxin and TEA and displayed slowed kinetics when co-expressed with  $\beta 1$  subunits. The extent to which any altered channel properties when compared to WT channels reflect the absence of allosteric input from the gating ring, revealing the baseline properties of the core, or reflect input from the 11 amino acid replacement tail is under investigation. Supported in part by NS061871 to LS and AR032805 to KLM.

## 2207-Plat

### Divalent Cation-Dependent Motion of the BK Channel Gating-Ring Reported by State Dependent FRET

Pablo Miranda<sup>1</sup>, Teresa Giraldez<sup>2</sup>, Miguel Holmgren<sup>1</sup>.

<sup>1</sup>NINDS, Bethesda, MD, USA, <sup>2</sup>Research Division, HUNSC, Tenerife, Spain.

Large conductance voltage- and calcium-dependent potassium channels (BK) are important controllers of cell excitability. The channel's open probability is regulated by changes in transmembrane voltage, intracellular calcium and magnesium concentrations<sup>1</sup>. The voltage sensor resides within the transmembrane region of the channel. Divalent cation binding is sensed by the intracellular C-terminal "gating ring", formed by eight Regulator of Conductance for  $\text{K}^{+}$  (RCK) domains<sup>2</sup>. Using patch-clamp fluorometry we have recently shown that remarkable large rearrangements of the gating ring occur upon  $\text{Ca}^{2+}$  binding in intact BK channels<sup>3</sup>, much larger than those predicted by existing X-ray structures of the isolated gating ring<sup>2</sup>. Using the same technical approach, we have now explored the conformational changes of the gating ring in intact channels induced by other divalent cations ( $\text{Mg}^{2+}$  and  $\text{Ba}^{2+}$ <sup>4,5</sup>) in relation with